International Journal of Pharmaceutics 414 (2011) 298–311

Contents lists available at ScienceDirect

International Journal of Pharmaceutics

journal homepage: www.elsevier.com/locate/ijpharm

Pharmaceutical Nanotechnology

Nanostructure formation in aqueous solution of amphiphilic copolymers of 2-(*N*,*N*-dimethylaminoethyl)methacrylate and alkylacrylate: Characterization, antimicrobial activity, DNA binding, and cytotoxicity studies

Pranabesh Dutta [a], Joykrishna Dey [a,*], Anshupriya Shome [b,1], Prasanta Kumar Das [b,**]

[a] *Department of Chemistry, Indian Institute of Technology, Kharagpur 721302, India*
[b] *Department of Biological Chemistry, Indian Association for the Cultivation of Science, Jadavpur, Kolkata 700032, India*

ARTICLE INFO

Article history:
Received 12 March 2011
Received in revised form 1 May 2011
Accepted 2 May 2011
Available online 11 May 2011

Keywords:
Hydrophobically modified polymer
Transmission electron microscopy
Antimicrobial activity
DNA binding
Biocompatibility

ABSTRACT

Three amphiphilic random copolymers poly(2-(dimethylaminoethyl)methacrylate-co-alkylacrylate) (where, alkyl = hexyl, octyl, dodecyl) with 16 mol% hydrophobic substitution were synthesized. Surface tension, viscosity, fluorescence probe, dynamic light scattering (DLS), as well as transmission electron microscopic (TEM) techniques were utilized to investigate self-assembly formation by the hydrophobically modified polymers (HMPs) in pH 5. Formation of hydrophobic domains through inter-polymer chain interaction of the copolymer in dilute solution was confirmed by fluorescence probe studies. Average hydrodynamic diameter of the copolymer aggregates at different polymer concentration was measured by DLS studies. The copolymer with shorter hydrophobic chain exhibits larger hydrodynamic diameter in dilute solution, which decreased with either increase of concentration or increase of hydrophobic chain length. TEM images of the dilute solutions of the copolymers with shorter as well as with longer hydrophobic chain exhibit spherical aggregates of different sizes. The antimicrobial activity of the copolymers was evaluated by measuring the minimum inhibitory concentration value against one Gram-positive bacterium *Bacillus subtilis* and one Gram-negative bacterium *Escherichia coli*. The copolymer with the octyl group as pendent hydrophobic chain was found to be more effective in killing these microorganisms. The interaction of the cationic copolymers with calf-thymus DNA was studied by fluorescence quenching method. The polymer-DNA binding was found to be purely electrostatic in nature. The hydrophobes on the polymer backbone were found to have a significant influence on the binding process. Biocompatibility studies of the copolymers in terms of cytotoxicity measurements were finally performed at different concentrations of the HMPs to evaluate their potential application in biomedical fields.

1. Introduction

Water-soluble cationic polymers have been the subject of continuing investigation over the years. These have received great attention due to their important role in biomedical applications, especially as carriers for controlled drug release (Zhang et al., 2008), scaffolds for tissue engineering (Malafaya et al., 2007), and vehicles for gene transfer therapy (Lv et al., 2006; Park et al., 2006). Various cationic copolymers like poly(L-lysine) (Niwa et al., 2002), polyethylenimine (PEI) (Lungwitz et al., 2005), and derivatives of chitosan (Kim et al., 2007), have been synthesized and studied for the same. One additional attractive feature for these cationic copolymers is their ability of killing pathogenic microorganisms and acting as an antimicrobial agent which can be used in areas such as healthcare products, food storage, water purification systems, household sanitation, medical devices, etc. These are mostly nonvolatile, chemically stable, and more efficient in comparison to the commonly used low-molecular-weight antimicrobial agents (Kawabata, 1992; Tashiro, 2001). As a result, continuous efforts have been made for the last few years to develop polycations with antimicrobial function (i.e. polymeric biocides). The mechanism of antimicrobial activity depends largely on the hydrophilic–hydrophobic balance. Since the long chain hydrophobic functionalities provide a compatibility with the lipid bilayer of the bacterial cytoplasmic membrane, it is important to have optimum/thresholds hydrophobic functionalities for diffusion through the cell membrane (Ikeda et al., 1986; Nonaka et al., 2003). Based on this background several hundred to thousands of polymeric compounds with varying lipophilic–lipophobic balances have been synthesized and tested for different microbes

* Corresponding author. Tel.: +91 3222 283308; fax: +91 3222 255303.
** Corresponding author. Tel.: +91 33 2473 4971; fax: +91 33 2473 2805.
E-mail address: joydey@chem.iitkgp.ernet.in (J. Dey).
[1] Tel.: +91 33 24734971; fax: +91 33 24732805.

0378-5173/$ – see front matter © 2011 Elsevier B.V. All rights reserved.
doi:10.1016/j.ijpharm.2011.05.006

(Kenawy et al., 2007; Palermo et al., 2009). However, it has been found that the antimicrobial activities of polycations having similar structures can vary dramatically and there is no such strict structure–property relationship for the cationic polymers. One possible reason behind this heterogeneity might be due to the polydisperse nature of the polymers with varying range of molecular weights (Kanazawa et al., 1993). In fact, the average molecular weight of polymers plays a substantial role in governing the biological function especially microbial activity, toxicity, etc.Among various other water-soluble cationic polymers investigated so far, poly(2-(dimethylaminoethyl)methacrylate, poly(DMAEMA) is one such polymer that has gained potential application starting from drug/gene delivery to water purification systems (Van de Wetering et al., 1997; Gu et al., 2009; Hoogeveen et al., 1996; Zhu et al., 2009; Keely et al., 2009). This is a weak polyelectrolyte with p$K_a \approx 7.9$ (Merle, 1987; Pradny and Sevcik, 1985) in water, which is close to the physiological pH and shows lower critical solution temperature, LCST, behavior quite similar to PNIPAM. Depending on the molecular weight, pH, and salt concentration various values in the range of 38–50 °C have been reported for its LCST in aqueous media (Lee et al., 2003). In regards to their application as antimicrobial agents it has been demonstrated that this homopolymer can inhibit the growth of *Escherichia coli* and *Bacillus subtilis* when attached to glass (Lee et al., 2004; Huang et al., 2008), filter paper (Lee et al., 2004; Roy et al., 2008), polystyrene (Lenoir et al., 2005), and polypropylene (Huang et al., 2007). Very recently, Rawlinson et al. (2010) have carried out a detailed investigation on the antibacterial activity of unconjugated and 50% conjugated poly(DMAEMA) polymer against a range of bacterial strain. They have found that poly(DMAEMA) acts as bacteriostatic against Gram-negative bacteria with MIC values between 0.1 and 1 mg/mL. They observed that in case of Gram-negative bacteria it is active around its pK_a and at higher pH values, while for Gram-positive bacteria the poly(DMAEMA) is active around its pK_a and at lower pH values.

The poly(DMAEMA) homopolymer has also been established as an efficient gene carrier (Wetering et al., 1998). It binds plasmid DNA resulting polymer/plasmid complexes (commonly known as polyplexes) and introduces DNA into cells. The lower pK_a value of poly(DMAEMA) amino groups is believed to contribute to its high transfection efficiency (Wetering et al., 1999). The transfection efficiency of poly(DMAEMA) can further be modulated with incorporation of hydrophilic or hydrophobic functional group into this polymer. Consequently, various hydrophilic/hydrophobic monomers were polymerized with DMAEMA to investigate their transfection properties (Tan et al., 2006; Rungsardthong et al., 2001). The hydrophobic monomers lead to stable complex formation with DNA for efficient cell uptake and prevent enzymatic degradation of DNA. This causes higher transfection efficiency than polymer systems using only ionic interactions. Kurisawa and coworkers observed that in the case of water-soluble terpolymer poly(*N*-isopropylacrylamide (IPAAm)-*co*-2-(dimethylamino)ethyl methacrylate (DMAEMA)-*co*-butylmethacrylate (BMA)) containing 20 mol% of DMAEMA, the transfection efficiency with 0, 2, and 5 mol% of BMA was low. However, when the BMA content increases to 10 mol%, a 2-fold higher transfection efficiency than that of the poly(DMAEMA) control homopolymer can be achieved (Kurisawa et al., 2000).

Although the antimicrobial activity of poly(DMAEMA) has been investigated either in its unconjugated or quaternized ammonium form, to our knowledge, there is hardly any systematic report of the microbial activity, toxicity, and self-assembly properties for this polymer with hydrophobic side chain of different chain length. Introduction of hydrophobic monomer units onto the poly(DMAEMA) backbone will create an amphiphilic structure in which hydrophilic/hydrophobic ratio will govern the biocidal activity of the copolymers and much less amount of compound will

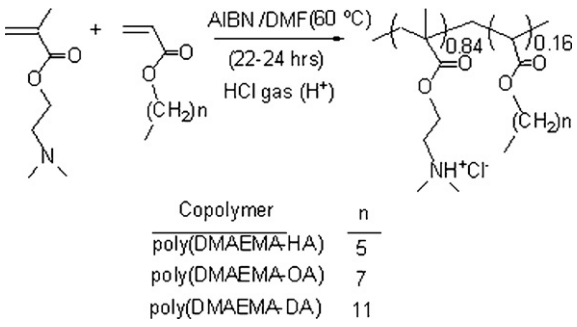

Fig. 1. Synthetic scheme for the preparation of cationic copolymers reported in this work.

be required for killing those pathogenic microorganisms. Moreover, the detailed self-assembly studies along with the evaluation of antimicrobial activity, DNA binding ability, and toxicity will open up opportunities for their use in other areas also. Therefore, in this article we have extended the strategy to introduce hydrophobic modification of DMAEMA based polyelectrolyte with different hyhdrophobic side chain. Three random copolymers of DMAEMA and alkylacrylate (where alkyl = hexyl, octyl, dodecyl) with 16 mol% hydrophobic substitution (Fig. 1) were synthesized and their self-assembly properties were studied in terms of intra- and intermolecular interaction in aqueous media combining surface tension, viscometry, fluorescence, dynamic light scattering (DLS), and transmission electron microscopy (TEM) techniques. Effects of concentration, pH, electrolyte, and temperature have been investigated on the aggregation behavior of these hydrophobically modified polyelectrolytes (HMPs). Finally, antimicrobial activity, DNA binding ability, and toxicity measurements were performed to explore the potential applications of these copolymers.

2. Experimental

2.1. Materials

The monomer 2-(*N*, *N*-dimethylaminoethyl)methacrylate (DMAEMA) (Aldrich) was purified by reported procedure (Georgiou et al., 2005). Dodecanol, octanol, hexanol (SRL), acryloyl chloride, chloroform-d ($CDCl_3$), deuterium oxide (D_2O), and 3-(4,5-dimethyl-2-thiazolyl)-2,5-diphenyl-2H-tetrazolium bromide (MTT) (Aldrich) were used without further purification. The radical initiator 2,2′-azobis(isobutyronitrile), AIBN (Aldrich) was recrystallized from methanol. The fluorescence probes, such as pyrene, 1,6-diphenyl-1,3,5-hexatriene (DPH), and *N*-phenyl-1-naphthylamine (NPN) (Aldrich) were recrystallized from ethanol or acetone-ethanol mixture three times before use. Calf-thymus deoxyribonucleic acid (Ct-DNA) (SRL, Mumbai) and ethidium bromide (SRL, Mumbai) were used as received. Analytical grade sodium hydroxide, sodium bicarbonate, sodium hydrogen phosphate, sodium dihydrogen phosphate, sodium chloride and hydrochloric acid were used directly from the bottle. All the solvents, ethanol, methanol, tetrahydrofuran (THF), acetone, and dichloromethane were of commercially available and were dried and distilled fresh before use. Doubly distilled water was used for preparation of all solution.

2.2. Synthesis of monomers

Dodecylacrylate (DA), octylacrylate (OA), and hexylacrylate (HA) were prepared by acylation of the respective alcohol with acryloyl chloride in a manner analogous to the synthesis of *N*-alkylacrylamide reported by Morishima et al. (Morishima et al., 1989). Briefly, in a 100 mL round-bottom flask fitted with mag-

netic stirrer *n*-alkanol (0.01 mol) was dissolved in 10 mL of THF. A solution of triethylamine (0.01 mol) in 10 mL of THF was then added. The reaction mixture was cooled in an ice bath below 10 °C. Acryloyl chloride (0.012 mol) was added drop wise into the mixture. After the addition, the solution was stirred with magnetic stirrer for additional 3 h at room temperature. The reaction mixture was poured into water and extracted with dichloromethane. The organic layer was washed three times with water and dried over anhydrous magnesium sulfate. After evaporation of the solvent the residue was purified by column chromatography using silica gel and was identified by elemental analysis, ^{1}H NMR, and FT-IR spectroscopy.

2.2.1. Dodecylacrylate (DA)

(Yield 84%) FT-IR (KBr, cm^{-1}): 2926, 2855 (C–H stretching); 1729 (C=O stretch of ester); 1637 (–C=C-stretching); 1466, 1407, 1271, 1191; **1**H NMR (200 MHz, $CDCl_3$), ((δ in ppm): 6.41 (dd, 1H, H_2C=C*H*), 6.18 (dd, 1H, H*H*C=CH–), 5.81 (dd, 1H, *H*HC=CH–), 4.21 (t, 2H, O–CH_2–CH_2–), 1.67 (m, 2H, O–CH_2–CH_2–$(CH_2)_9$–CH_3), 1.29 (m, 18H, O–CH_2–CH_2–$(CH_2)_9$–CH_3), 0.80 (t, 3H, O–CH_2–CH_2–$(CH_2)_9$–CH_3); *CHN analysis*: calcd. (%): C, 74.94, H, 11.74; found: C, 74.37, H, 11.17.

2.2.2. Octylacrylate (OA)

(Yield 79%) FT-IR (KBr, cm^{-1}): 2922, 2852 (C–H stretching); 1727 (C=O stretch of ester); 1630 (–C=C-stretching); 1462, 1404, 1263, 1189; ^{1}H NMR (200 MHz, $CDCl_3$), ((δ in ppm): 6.35 (dd, 1H, H_2C=C*H*), 6.10 (dd, 1H, H*H*C=CH–), 5.80 (dd, 1H, *H*HC=CH–), 4.14 (t, 2H, O–CH_2–CH_2–), 1.64 (m, 2H, O–CH_2–CH_2–$(CH_2)_5$–CH_3), 1.32 (m, 10H, O–CH_2–CH_2–$(CH_2)_5$–CH_3), 0.85 (t, 3H, O–CH_2–CH_2–$(CH_2)_5$–CH_3); *CHN analysis* calcd. (%): C, 71.69, H, 10.93; found: C, 71.55, H, 11.17.

2.2.3. Hexylacrylate (HA)

(Yield 81%) FT-IR (KBr, cm^{-1}): 2932 (C–H stretching); 1723 (C=O stretch of ester); 1633 (–C=C-stretching); 1458, 1404, 1271, 1190; ^{1}H NMR (200 MHz, $CDCl_3$), ((δ in ppm): 6.38 (dd, 1H, H_2C=C*H*), 6.09 (dd, 1H, H*H*C=CH–), 5.79 (dd, 1H, *H*HC=CH–), 4.11 (t, 2H, O–CH_2–CH_2–), 1.63 (m, 2H, O-CH_2-CH_2-$(CH_2)_3$-CH_3), 1.34 (m, 6H, O–CH_2–CH_2–$(CH_2)_3$-CH_3), 0.87 (t, 3H, O–CH_2–CH_2–$(CH_2)_3$–CH_3); *CHN analysis*: calcd. (%): C, 69.19, H, 10.32. Found: C, 68.87, H, 10.56.

2.3. Synthesis of copolymers

The three tertiary amine-based cationic HMPs were prepared by copolymerization of DMAEMA and alkylacrylate (16 mol%), similar to the synthetic pathway reported recently by our group (Dutta et al., 2009). Briefly, DMAEMA and alkylacrylate (HA, OA or DA) were dissolved in DMF with pre-determined weight ratio. Oxygen-free nitrogen was purged through the solution mixture for 45 min at 60 °C. AIBN (1 mol% of the total monomer concentration) dissolved in DMF was added via syringe. The polymerization was continued for 24 h. Finally, it was recovered by passing dry HCl gas through the reaction mixture. For complete precipitation, the mixture was poured into large excess of chloroform. To purify the copolymers, repeated precipitation from methanol with chloroform was done and the product was finally dissolved in pure water. Subsequently, the solution was dialyzed (MWCO 12,000–14,000 g/mol) against distilled water (pH 6–7) for 1 week and then lyophilized. The copolymers were chemically identified by FT-IR and ^{1}H NMR spectroscopy. The synthetic scheme of polymerization reaction is presented in Fig. 1. Conveniently, the HMPs with different hydrophobe chain length (6, 8, and 12) were abbreviated as follows: poly(DMAEMA-HA), poly(DMAEMA-OA), and poly(DMAEMA-DA).

2.3.1. Poly(2-(dimethylaminoethyl)methacrylate-co-hexylacrylate) [poly(DMAEMA-HA)]

FT-IR (KBr, cm^{-1}): 3411 (N–H stretching), 2932, 2837 (alkyl C–H stretching), 1728 cm^{-1} (C=O stretch, ester group), 1259 cm^{-1} (C–N stretching),^{1}H NMR (200 MHz, $CDCl_3$ + CD_3OD (20 μL)), ((δ in ppm): 4.31 (br, 2H, –O–CH_2–CH_2–NH$(CH_3)_2$, DMAEMA), 2.85 (br, 6H, –O–CH_2–CH_2–NH(C$H_3)_2$, DMAEMA), 1.64 (br, 6H, –O–CH_2–CH_2–$(CH_2)_3$–CH_3, HAc), 0.84 (m, 3H, –O–CH_2–CH_2–$(CH_2)_3$–CH_3, HAc), 1.83 (br, 1H, –C*H*–CH_2–, main chain), 2.54 (br, 2H, –C*H*–CH_2–, main chain).

2.3.2. Poly(2-(dimethylaminoethyl)methacrylate-co-octylacrylate) [poly(DMAEMA-OA)]

FT-IR (KBr, cm^{-1}): 3409 (N–H stretching), 2941, 2840 (alkyl C–H stretching), 1734 cm^{-1} (C=O stretch, ester group), 1257 cm^{-1} (C–N stretching), ^{1}H NMR (200 MHz, $CDCl_3$ + CD_3OD (20 μL)), ((δ in ppm): 4.39 (br, 2H, –O-CH_2–CH_2–NH$(CH_3)_2$, DMAEMA), 2.92 (br, 6H, –O–CH_2–CH_2–NH(C$H_3)_2$, DMAEMA), 1.72 (br, 6H, –O–CH_2–CH_2–$(CH_2)_5$–CH_3, OAc), 0.88 (m, 3H, –O–CH_2–CH_2–$(CH_2)_5$–CH_3, OAc), 1.94 (br, 1H, –C*H*–CH_2–, main chain), 2.58 (br, 2H, –C*H*–CH_2–, main chain).

2.3.3. Poly(2-(dimethylaminoethyl)methacrylate-co-dodecylacrylate) [poly(DMAEMA-DA)]

FT-IR (KBr, cm^{-1}): 3408 (N–H stretching), 2937 (alkyl C–H stretching), 1731 cm^{-1} (C=O stretch, ester group), 1260 cm^{-1} (C–N stretching), ^{1}H NMR (200 MHz, $CDCl_3$ + CD_3OD (20 μL)), ((δ in ppm): 4.28 (br, 2H, –O–CH_2–CH_2–NH$(CH_3)_2$, DMAEMA), 2.79 (br, 6H, –O–CH_2–CH_2–NH(C$H_3)_2$, DMAEMA), 1.58 (br, 6H, –O–CH_2–CH_2–$(CH_2)_9$–CH_3, DAc), 0.87 (m, 3H, –O–CH_2–CH_2–$(CH_2)_9$–CH_3, DAc), 1.87 (br, 1H, –C*H*–CH_2–, main chain), 2.51 (br, 2H, –C*H*–CH_2–, main chain).

2.4. General instrumentation

The ^{1}H NMR spectra were recorded on a Brucker SEM 200 spectrophotometer using $CDCl_3$ as solvent and trimethyl silane (TMS) as internal standards. For weighing of the samples, semi-micro-analytical balance (Sartorious, model: CP2225D) were used. The UV–vis spectra were recorded with a Shimazdu (model: 1601) spectrophotometer. The circular dichroism (CD) spectra were recorded with a Jasco J-810 spectropolarimeter using quartz cell of 10 mm path length. An average of four scan of each spectrum was taken under the conditions of 1-nm bandwidth, 2-s response time, and 50 nm/min scan speed. Each spectrum was corrected by subtracting the appropriate reference blank. The pH measurements were performed with a digital pH meter (pH 5652, EC India Ltd., Kolkata) using glass electrode. Average molecular weight and molecular weight distribution of the copolymers in their deprotonated form were obtained by gel permeation chromatography (GPC) using a Waters GPC instrument equipped with Styragel HR-4 columns. Tetrahydrofuran (THF) was used as an eluent (flow rate 0.6 mL/min). The molecular weight and polydispersity index were calculated from the calibration curve previously constructed from monodispersed polystyrene standard.

2.5. Surface tension measurement

To check the surface activity of the polymer, surface tension (γ) were measured in aqueous buffer solution of copolymer with a surface tensiometer (model 3S, GBX, France) using Du Nuöy ring detachment method. Before every measurement the platinum ring was cleaned properly with ethanol–HCl solution and checked the surface tension of distilled water. Aliquot of polymer stock solution made in buffer solution (pH 5) was gradually added to a beaker containing known volume of the same buffer and stirred gently

with a magnet. Before each measurement, the solution was allowed to stand for about 30 min to equilibrate at 30 °C and the mean of three measurements was taken as equilibrium surface tension.

2.6. Viscosity measurement

An Ubbelohde glass viscometer (ASTM-D-446) with efflux time of 180 s (for water) was used to measure the viscosity of aqueous polymer solutions. The sample as well as the viscometer was equilibrated at 30 °C throughout the experiment. At least five readings were taken to determine the average flow–through time of the copolymer solution at various concentrations (0.05–3 g/L). Specific viscosity was determined by comparison with the flow-through time of buffer alone. For determination of density of the copolymer solutions, a portable digital density meter (Densito 30 PX, Mettler-Toledo, GmbH) was used.

2.7. Steady-state fluorescence spectra

The steady-state fluorescence measurements of aqueous polymer solution containing pyrene (5.0×10^{-7} M) were performed on a SPEX Fluorolog-3 spectrofluorometer. A stock solution (1×10^{-3} M) in methanol was added to the polymer solution of different concentration, gently shaken and allowed to equilibrate for 24 h before measurement. The solutions were excited at 335 nm and the emission was recorded in the wavelength range 350–500 nm. The ratio of intensities of the first (I_1, at ~372 nm) and the third (I_3, at ~383 nm) vibronic peaks of the pyrene fluorescence spectrum was used as a measure of the polarity in the local environment. Stock solutions of NPN were prepared by adding the compound to buffer solution and stirring magnetically for 24 h. The excess compound was removed by filtration through Millipore syringe filter (0.22 μm) and the samples prepared with this stock solution were excited at 340 nm. The emission was collected in the range 360–550 nm after 24 h of equilibration. The excitation and emission slit widths of 2.5 and 2.5–4.0 nm, respectively, were used for the fluorescence measurements. The background spectra, either of the buffer alone or of the buffer containing HMP were subtracted from the corresponding sample spectra in all experiments.

A PerkinElmer LS-55 spectrophotometer equipped with filter polarizers that use the L-format configuration was used for fluorescence anisotropy measurements of DPH probe (details could be found elsewhere) (Roy et al., 2005). An average of six measurements was taken to calculate the final fluorescence anisotropy (r) value. The solution temperature of the samples was controlled by Thermo Neslab RTE-7 circulating water bath, which is connected directly to the magnetically stirred cell holder in the spectrometer.

2.8. Dynamic light scattering measurements

The dynamic light scattering (DLS) experiments were carried out on a home-built light scattering spectrophotometer (Dutta et al., 2009). The incident beam was generated from a vertically polarized 100 mW He–Ne laser source ($\lambda = 532$ nm) fixed at one arm of a goniometer, at varying scattering angles ($\theta = 50°, 70°, 90°, 100°$, and 120°). The scattered beam was counted by a photo-multiplier tube (PMT) detector, mounted on other arm of the goniometer. The output current from the PMT was then suitably amplified and digitized through various electronics before it was fed to a 256-channel digital correlator (7132 Malvern, UK) with 50 ns initial delay time. The temperature was set at 25 °C, unless changed to set other values. Prior to the measurement, each solution was cleaned by filtration through a 0.45 μm filter paper (Millipore Millex syringe filter). The final solution was loaded into an optical quality cylindrical quartz sample cell and placed in a borosilicate glass cuvette containing an index matching liquid (trans-decalene) at 25 °C for 30 min. The correlation curves obtained were analyzed using the CONTIN software provided by Malvern.

2.9. Transmission electron microscopy

The morphology of the copolymer aggregates in solution was investigated by transmission electron microscopy. The samples were prepared by immersing a 400 mesh size carbon-coated copper grid in to the copolymer solution (1 g/L) for 1 min. The excess liquid was blotted off with filter paper, air-dried, and kept in a moisture-free desiccators prior use. The measurements were carried on a JEOL-JEM 2100 (Japan) electron microscope operating at an accelerating voltage of 200 kV at room temperature.

2.10. Ethidium bromide displacement assay

The binding abilities of the cationic copolymers to ct-DNA were investigated by ethidium bromide displacement assay. A 500 μL of polymer solution of desired concentration (0.0005–0.016 g/L) was added into equal volumes of ct-DNA/EB solution to make final ct-DNA concentration of 0.01 g/L and EB concentration of 2.0×10^{-6} M to obtain polymer/DNA complexes with various weight ratios. Before measurement, the solutions were equilibrated for 12 h under dark condition. The final solutions were then excited at 530 nm and the emission was recorded in the wavelength range 500–700 nm.

2.11. Antimicrobial assay

In vitro antimicrobial activities of the cationic HMPs were evaluated using measurements of minimum inhibitory concentration (MIC) against both Gram-positive and Gram-negative bacteria. Gram-positive bacterium used in the present study was *B. subtilis*. While, Gram-negative strain investigated was *E. coli*. All the bacterial strains were procured from Institute of Microbial Technology, Chandigarh, India.

Culture conditions: Investigations of antibacterial activities were performed by both broth dilution and spread plate method (Pitt et al., 1994; Ikeda et al., 1984; Mitra et al., 2009; Roy and Das, 2008). The LB medium was utilized as a liquid medium that contained tryptone (10 g), yeast extract (5 g) and NaCl (10 g) in 1000 mL sterile distilled water at pH 7.0. Besides, LB agar that contained tryptone (10 g), yeast extract (5 g), NaCl (10 g) and agar (15 g) in 1000 mL of sterile distilled water of at pH 7.0 was used as a solid medium for spread plate study. The stock solutions of all the polymers as well as the required dilutions were made in autoclaved sterile water. For each bacterium, a representative single colony was picked up with a wire loop and that loop-full of culture was spread on LB agar slant to give single colony and incubated at 37 °C for 24 h. These fresh overnight cultures of all the bacteria were diluted as required to give a working concentration in the range of 10^6-10^9 colony forming units (cfu)/mL before every experiment.

Determination of minimum inhibitory concentration (MIC): The MIC is defined as the lowest concentration of an antimicrobial agent that will inhibit the growth of a microorganism after incubation. MIC values of HMPs were estimated by both broth dilution and spread plate method. MIC was measured using a series of test tubes containing the HMPs (0.05–200 μg/mL) in 5 mL LB broth. Diluted bacterial culture was added to each test tube in identical concentration, which was $7.5 \times 10^7 - 1 \times 10^8$ cfu/mL for *B. subtilis* and $3.75 \times 10^7 - 7.5 \times 10^7$ cfu/mL for *E. coli*. All the test tubes were then incubated at 37 °C for 24 h. The optical density of all the solutions was measured before and after incubation at 650 nm. The LB broth containing bacteria was used as a positive control. For comparison, both Gram-positive and Gram-negative bacteria were tested in broth supplemented with classical antibiotic streptomycin. All

the experiments were performed in triplicate and were repeated twice. The antimicrobial activity was also tested through spread plate method. For these experiments, an equal amount of bacterial culture was added to test tubes containing desired concentration of polymer solution in liquid LB medium. The test tubes were then inoculated at 37 °C for 5–7 h. Then, 50 μL from each tube was spread onto LB agar plates inside laminar flow. Finally, plates were incubated at 37 °C for 24 h, and the viable cells were counted.

2.12. Cytotoxicity assay

Cell culture: The 3T3 cell line (mouse fibroblasts) was grown in RPMI-1640 medium supplemented with 10% FBS, 2 mM L-glutamine, 100 units/mL penicillin, and 0.1 mg/mL streptomycin. Cells were grown in T-25 flasks at 37 °C, 5% CO_2 with a feeding cycle of 2 days. After cells became 80% confluent (after 2 days) they were trypsinized (0.25% Trypsin + 0.1% EDTA), centrifuged, and suspended in RPMI. Cells were washed twice and finally were frozen under liquid nitrogen in RPMI containing 10% dimethyl sulfoxide (DMSO) for future use. For subsequent passages, cells were seeded in fresh T-25 flasks at a density of 3×10^3 cells/cm^2 and were cultured in RPMI with a feeding cycle of 2 days.

MTT assay: The HMPs were dissolved in sterile water (pH 7.4) and filtered through 0.2 μm polycarbonate filter. Then the samples were diluted to desired concentrations. Cell suspensions were seeded into a 96-well plate at 3×10^3 cells/well in 0.1 mL complete medium. The cells were allowed to adhere and grow for 24 h at 37 °C in an incubator (Heraeus Hera Cell), after which the medium was aspirated and replaced with 0.1 mL fresh medium containing control and samples with the desired concentrations. After 48 h, the culture medium was removed, the cells were washed with sterile phosphate buffer saline (PBS) (0.1 mL/well) three times. Cell viability was assessed using a conventional MTT dye reduction assay. A 0.1 mL of MTT reagent in PBS (1 g/L) was added to each well. After 4–5 h incubation, the MTT reagent mixture was gently removed. Then 0.1 mL DMSO was added into each well to dissolve the purple formazan precipitate which was reduced from MTT by the viable cells with active mitochondria. The formazan dye was measured spectrophotometrically using benchmark microplate reader at 550 nm. All assays were performed in triplicate. The cytotoxic effect of each treatment was expressed as percent cell viability relative to the untreated control cells (% control) defined as:

$$\text{cell viability (\%)} = \frac{(\text{absorbance at 550 of treated cells with samples})}{(\text{absorbance at 550 of control cells without samples})} \times 100 \quad (1)$$

2.13. Hemolytic assay

The copolymers were dissolved in sterile water to desired concentrations (0.1 g/L, 1 g/L). Hemocompatibility was analyzed using the protocol reported by Katanasaka et al. (2008) with some modification. In brief, blood was obtained from 6-week-old BALB/c male mice and red blood cells (RBC) were collected by centrifugation (1500 rpm, 5 min, and 4 °C) of the blood. The collected RBC pellet was diluted in 20 mM HEPES buffered saline (pH 7.4) to give a 5% (v/v) solution. The RBC suspension was added to HEPES-buffered saline, 1% Triton X-100, and samples and incubated for 60 min at 37 °C. After centrifugation with Heraeus table top centrifuge 5805R at 12,000 rpm at 4 °C, the supernatants were transferred to a 96-well plate. Hemolytic activity was determined by measuring the absorption at 550 nm using benchmark microplate reader (Biorad Microplate reader 5804R). The samples with 0% lysis (HEPES buffer saline) and 100% lysis (1% Triton X-100) were referred as $^+$Ve and $^-$Ve control, respectively. All assays were performed in triplicate.

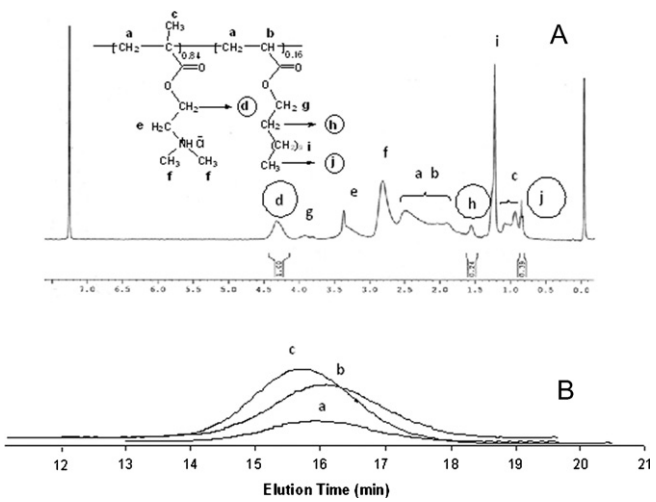

Fig. 2. (A) ^{1}H NMR spectra of typical poly(DMAEMA-DA) copolymer in $CDCl_3$ (with 30 μL CD_3OD in 0.5 mL); (B) GPC chromatograms of (a) poly(DMAEMA-HA), (b) poly(DMAEMA-OA), (c) poly(DMAEMA-DA).

Hemolytic effect of each treatment was expressed as percent cell lysis relative to the untreated control cells (% control) defined as:

$$\text{hemolysis (\%)} = \frac{(\text{Abs at 550 samples} - \text{Abs at 550 }^-\text{Ve control})}{(\text{Abs at 550 }^+\text{Ve control} - \text{Abs at 550 }^-\text{Ve control})} \times 100 \quad (2)$$

2.14. Statistical analysis

The statistical method used to analyze the significant differences between control and treatment groups is one-way analysis of variance (ANOVA). The results were expressed as mean ± SD unless otherwise noted; $p < 0.001$ was considered statistically significant.

3. Results and discussion

3.1. Molecular characterization of the copolymers

To demonstrate the successful syntheses of the random copolymers FT-IR, and ^{1}H NMR spectra were studied. Disappearance of the C=C bond stretching frequency (1610 cm^{-1}) of the acrylate monomers in the FT-IR spectrum (not shown here) indicates the formation of polymeric structures. This was further confirmed by the absence of the vinylic proton signal along with broad peaks in the ^{1}H NMR spectrum. A representative ^{1}H NMR spectrum of poly(DMAEMA-DA) is presented in Fig. 2(A). The signals at 4.3 and 2.8 ppm correspond, respectively, to the proton bonded to the carbon adjacent to oxygen (br, 2H, –O–CH_2–CH_2–NH(CH_3)$_2$) and to the methyl groups attached to nitrogen (br, 6H, –O–CH_2–CH_2–NH(CH_3)$_2$) of the DMAEMA monomer. The peaks of the DA monomer are observed at 1.6 ppm (br, 18H, –O–CH_2–CH_2–(CH_2)$_9$–CH_3), and 0.8 ppm (m, 3H, –O–CH_2–CH_2–(CH_2)$_9$–CH_3). The signals corresponding to the methylene and methyne protons on the main chain are observed from 1.8 to 2.5 ppm. The integrated signals at 4.3 ppm for DMAEMA, and either of 1.6 ppm or 0.8 ppm for DA were employed to calculate the mole fraction of the two monomers in the copolymer. The results agree very well with the feed composition, taking the experimental error (±5%) of the method into account.

The GPC experiment was performed to measure the molar masses of the copolymers. Representative overlaid GPC chromatogram traces of poly(DMAEMA-HA), poly(DMAEMA-OA), and

Table 1
Copolymer composition, molecular weights, and polydispersity index (PDI), intrinsic viscosity ([η]), and limiting surface tension (γ_{min}) of the copolymers.

Copolymer	$M_w/10^4$ (g/mol)	$M_n/10^4$ (g/mol)	PDI	[η] (L/g)	γ_{min} (mN/m)
Poly(DMAEMA-HA)	6.38	4.34	1.47	0.102	55.1
Poly(DMAEMA-OA)	6.75	4.19	1.61	0.162	52.7
Poly(DMAEMA-DA)	7.19	4.70	1.53	0.202	50.3

poly(DMAEMA-DA) have been shown in Fig. 2(B). All three copolymers exhibit unimodal molecular weight distribution. The average molecular weight and polydispersity index (PDI) obtained are summarized in Table 1. The data in Table 1 suggest that the HMP with longer hydrophobic chain has higher molecular weight compared to the copolymer of shorter hydrophobic chain analog.

Aqueous solutions of the HMPs became turbid beyond pH 9. Increased hydrophobicity of these copolymers is likely responsible for the precipitation from aqueous solution at higher pH. The HMPs are hydrochloride salts of the corresponding polymer containing tertiary amine group along its backbone. As mentioned earlier the average pK_a value of the ammonium groups of poly(DMAEMA) as reported in the literature is ~7.9 (Merle, 1987; Pradny and Sevcik, 1985). This means that in neutral pH the HMPs exist in the partially protonated form, whereas in pH < 7.0 the amine groups are expected to be completely ionized. The change in pH can therefore change the conformation of the HMPs in solution and has been discussed below. In their partially charged form at neutral pH the HMPs are expected to remain in the conformation that favors intra-polymer aggregation producing unimolecular micelles. On the other hand, in their fully ionized form in pH < 7.0, they are expected to behave either like polyelectrolytes or to undergo inter-polymer aggregation. Such conformational changes of the copolymers can be used in pH-triggered intracellular delivery of drugs and DNA by exploitation of intracellular pH gradients which varies between 4.5 and 8 among different organelles (cytoplasm, endosomes, lysosomes, endoplasmic reticulum, mitochondria, and nuclei) (Asokan and Cho, 2002). For this reason, we have studied their physicochemical properties in pH 5 to ensure complete ionization of the amine groups.

3.2. Surface activity and solution viscosity of the HMPs

Because of the amphiphilic character, the HMPs are expected to possess surface-active properties. This was evaluated by monitoring the equilibrium surface tension (γ) of water at different polymer concentrations. As observed in Fig. S1 of "supplementary material", the surface tension of water, γ decreases with increase in concentration indicating their amphiphilic character. The γ_{min} values of the HMPs are included in Table 1. The data suggest that the amphiphilicty increases with the increase of chain length of the hydrophobe unit.

The variation of reduced viscosity (η_{sp}/C) with the polymer concentration in aqueous buffer solution (pH 5) has been shown in Fig. S2 of "supplementary material". All the copolymers exhibit a typical polyelectrolyte behavior in dilute solution. That is the η_{sp}/C value increased with decreasing (copolymer) due to the expansion of the macroion chain, which is caused by the intra- and inter-molecular repulsive interactions among the ionized groups along the chain. Reduced viscosity values, at the same polymer concentration are seen to increase in the order: poly(DMAEMA-HA) < poly(DMAEMA-OA) < poly(DMAEMA-DA), which means for a constant degree of polymerization, with increasing the hydrophobic chain length a higher content of the cationic units in the copolymer is responsible for an increase of the coil dimension. To obtain intrinsic viscosity [η] value the curves shown in Fig. S2 of "supplementary material" were linearized applying Fuöss equation:

$$\frac{\eta_{sp}}{C} = \frac{[\eta]}{1 + kC^{0.5}} \quad (3)$$

where η_{sp}, C [η] and k are the specific viscosity, the concentration of the polymer, the intrinsic viscosity, and Fuöss constant, respectively. Viscometric data obtained in terms of the Fuöss equation are presented in the inset of Fig. S2 of "supplementary material". As can be observed straight lines are obtained for both the samples over a wide range of concentration allowing us to calculate the intrinsic viscosity values. The intrinsic viscosity values determined using Fuöss method is presented in Table 1. It is observed that [η] value is higher for the polymer with longer hydrophobic chain length. This is quite reasonable since the viscosity reflects the polymer size, larger the size of the polymer, higher is the viscosity.

3.3. pH dependent self-aggregation of the HMPs

The copolymers are carrying tertiary amine groups along their backbone. It is therefore obvious that the conformation of the HMPs poly(DMAEMA-HA), poly(DMAEMA-OA), and poly(DMAEMA-DA) should be a function of the solution pH. The pH dependent conformational transition was monitored by measuring the spectrum of NPN fluorescence in the presence of copolymers at different solution pH. The fluorescence emission spectrum of NPN is known to depend on the environment of the system. Generally, a very weak fluorescence is detected in aqueous medium with emission maximum (λ_{max}) at 460 nm which gets blue shifted accompanied by a huge increase of fluorescence intensity in going from water to less polar solvent. The detailed spectral properties of this hydrophobic probe have been reported in our earlier publications (Dutta et al., 2009; Mohanty and Dey, 2007). The shift of emission maximum ($\Delta\lambda = \lambda_{max}(\text{water}) - \lambda_{max}(\text{polymer})$) and the change in relative intensity (I/I_o) are shown in Fig. 3. As seen, both $\Delta\lambda$ (Fig. 3(a)) and I/I_o ((Fig. 3(b)) increases in going from lower to higher pH. The feature of the curves is nearly sigmoid. Although a large change in $\Delta\lambda$ was observed for copolymers poly(DMAEMA-HA) and poly(DMAEMA-OA), much less change can be found for the copolymer poly(DMAEMA-DA). At low pH (<7.0), the amine groups become protonated thus increasing the overall charge along the backbone. As a result, the hydrophobic interaction among the long chain alkyl groups is weakened by the charge repulsion causing release of the probe to bulk water. In other words, the aggregate structures are disrupted as a result of lowering the pH. However, at higher pH (>7.0) the free amine groups become less protonated and the hydrophobic character along the chain becomes stronger. Consequently, a large fraction of the probe molecules further partitioned into the hydrophobic microenvironments. It is quite evident from the plots of both figures that all the three HMPs have a phase transition around pH 6.0 and may be taken as the average pK_a value of the tertiary amine groups. Therefore, the zeta-potential (ζ) measurement was performed for the copolymers at pH 5.0 for 1 g/L copolymer solution and the data are summarized in Table 2. The positive potential values clearly suggest that the polymers are positively charged.

3.4. Self-assembly behavior and microenvironments of the aggregates

To obtain information about the aggregation properties of the HMPs, steady state fluorescence probe studies were carried out next in aqueous solution of pH 5 using NPN, pyrene, and DPH as probe molecules. The fluorescence spectra of NPN were further measured in the presence of different polymer concentration. The emission maximum of NPN undergoes a blue shift accom-

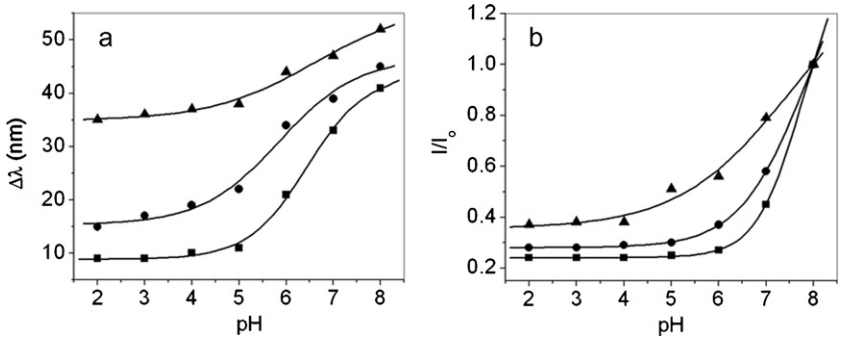

Fig. 3. Plots of (a) $\Delta\lambda$, and (b) I/I_o of NPN probe as a function of pH in the presence of 0.25 g/L copolymer solution at 30 °C: (■) poly(DMAEMA-HA), (●) poly(DMAEMA-OA), and (▲) poly(DMAEMA-DA).

Table 2
Physico-chemical properties of the copolymers (1 g/L) in aqueous acetate buffer solution (pH 5).

Copolymer	CAC[a] (g/L)	$\Delta\lambda$[b] (nm)	I_1/I_3[b]	r[c]	$\langle R_h \rangle$[d] (nm)	ζ[e] (mV)
Poly(DMAEMA-HA)	0.0455	17	1.69	0.178	16, 223	+32.2
Poly(DMAEMA-OA)	0.0366	24	1.6	0.184	14.5, 158	+28.3
Poly(DMAEMA-DA)	0.0169	31	1.42	0.197	8, 140	+24.5

[a] Critical aggregation concentration (CAC).
[b] Micropolarity ($\Delta\lambda$ and I_1/I_3).
[c] Viscosity (r).
[d] Mean hydrodynamic diameter $\langle R_h \rangle$.
[e] Zeta potential (ζ).

panied by a rise in fluorescence intensity in the presence of increasing concentration of copolymer, indicating partitioning of NPN into the hydrphobic domains. The shifts of emission maximum ($\Delta\lambda$) determined at different polymer concentrations are plotted in Fig. 4(a). Both the relative fluorescence intensity (I/I_o) (not shown), and $\Delta\lambda$ was found to increase with increase in polymer concentration. As can be seen in Fig. 4(a), a concentration-independent regime of $\Delta\lambda$ value appeared in all cases. However, with the increase in polymer concentration the value of $\Delta\lambda$ gradually increases. The concentration corresponding to the inflection point of the plots as indicated in Fig. 4(a) was therefore taken as CAC. The CAC value thus obtained are presented in Table 2. The CAC values are in the order poly(DMAEMA-HA) > poly(DMAEMA-OA) > poly(DMAEMA-DA). This is just opposite to the order of molecular weights of the copolymers. The $\Delta\lambda$ value, which is a measure of the hydrophobicity of the aggregates was determined at a given concentration (1.0 g/L) of the all the copolymer solutions. The data listed in Table 2 show that hydrophobicity increases with the increase of molecular weight. The formation of hydrophobic domains at very low concentration was also confirmed by measuring the micropolarity of the aggregates using pyrene. The I_1/I_3 ratio determined in the concentration range 1×10^{-4} to 4 g/L for all the HMPs are presented in the inset of Fig. 4(a). It is observed that above a certain concentration, the I_1/I_3 ratio decreases sharply, indicating intermolecular interaction. The concentration corresponding to the inflection point of the sigmoidal curves in the inset of Fig. 4(a) are close to the value obtained from the fluorescence titration of NPN and can therefore be regarded as CAC. The I_1/I_3 value (~1.35) obtained for poly(DMAEMA-DA) at the limiting concentration is very similar to those observed for CTAC or CTAB surfactant micelles (Kalyanasundaram, 1987). The I_1/I_3 value in 1 g/L polymer solution is given in Table 2. The I_1/I_3 value of the HMPs decreases with the increase of hydrophobe chain length, which is consistent with the increase of $\Delta\lambda$ value of the NPN probe.

To further investigate the microenvironment of the copolymer aggregates and its relation with the hydrophobic chain length, fluorescence intensity as well as fluorescence anisotropy (r) measurements were performed employing DPH probe. The DPH is almost insoluble in water and thus weakly fluorescent. However, its fluorescence intensity is greatly enhanced upon solubilization in

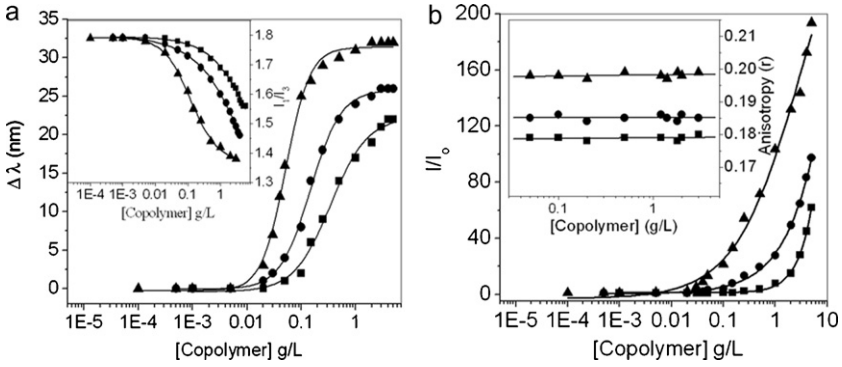

Fig. 4. (a) Plots of emission maximum shift ($\Delta\lambda = \lambda_{max}(\text{water}) - \lambda_{max}(\text{polymer})$), of NPN versus polymer concentration at 30 °C. (Inset: Plot of intensity ratio (I_1/I_3) of pyrene against polymer concentration]; (b) Plots of relative fluorescence intensity (I/I_o) of DPH probe in different polymer concentration at 30 °C (Inset: Variation of fluorescence anisotropy (r) of DPH probe with the concentration; (■) poly(DMAEMA-HA), (●) poly(DMAEMA-OA), and (▲) poly(DMAEMA-DA).

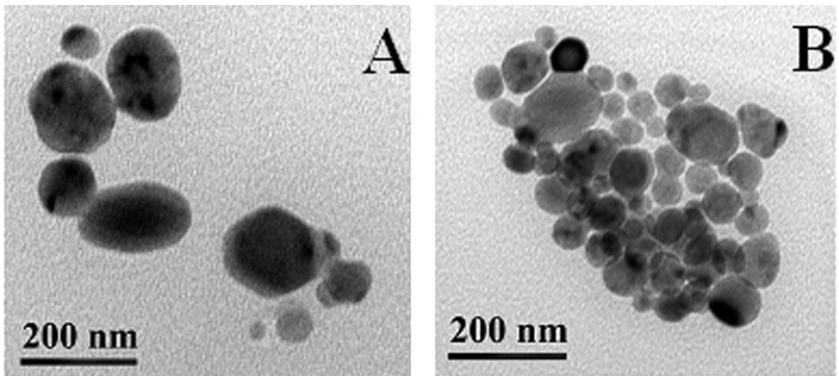

Fig. 5. TEM images (unstained) of 1 g/L (A) poly(DMAEMA-HA) and (B) poly(DMAEMA-DA) in acetate buffer of pH 5.

the hydrophobic microdomains of micelles. Therefore, the intensities of DPH fluorescence were measured at an emission wavelength of 450 nm in aqueous copolymer solution and were compared with the intensity of DPH in water. In poly(DMAEMA-DA), the relative intensity (I/I_o) increases considerably with the increase of polymer concentration (Fig. 4(b)). However, the increase is much less at the same polymer concentration for poly(DMAEMA-HA), and poly(DMAEMA-OA). These observations also signify the partitioning of DPH into the hydrophobic microdomains formed through association of pendent alkyl chains of the copolymers. Here also, a concentration-independent region was observed which further substantiate the intermolecular association of the copolymers. The rotational motion of DPH molecule usually becomes restricted when it is solubilized into the hydrophobic core of the aggregate. This is evident by the high *r*-values of DPH in solutions of the HMP at concentrations above the respective CAC value. The plots of *r* as a function of (copolymer) have been shown in the inset of Fig. 4(b). As observed, the *r*-value is independent of polymer concentration above CAC. The *r*-values in 1 g/L polymer solution are listed in Table 2. It is important to note that the *r*-values for all the three polymers at any polymer concentration above CAC is very high and increases with the increase of hydrophobe chain length, suggesting tighter packing of the hydrophobes in the aggregate with the increase of chain length. This restricts the motion of the DPH molecule resulting in a high value of *r*. The constant value of *r* at higher polymer concentrations might be due to the aggregation of smaller aggregates forming larger aggregates.

3.5. Microstructure of the aggregates

The morphology of the aggregates formed by the HMPs in aqueous solution was visualized by TEM technique. The images of the unstained samples (1 g/L) of poly(DMAEMA-HA), and poly(DMAEMA-DA) have been presented in Fig. 5. In both cases, the spheroid morphology of the copolymer aggregates is clearly visible. The sizes of the micelles observed for poly(DMAEMA-HA) are larger (~100–150 nm) than those formed by poly(DMAEMA-DA). However, with poly(DMAEMA-DA) a large number of smaller aggregates of different sizes are visible, and owing to the stronger interaction among hydrophobes they seem to be merging together. The particles, as expected, are positively charged, which is confirmed by the zetapotential (ζ) values (Table 2).

3.6. Hydrodynamic diameter of the aggregates

Dynamic light scattering experiments were performed to measure the effective hydrodynamic radii and the population (in terms of size) of the aggregates formed by the HMPs. Fig. 6(a) illustrates the histograms of size distribution of 2 g/L copolymer in pH 5 containing 100 mM NaCl. For all the three HMPs, a bimodal size distribution was observed. As seen from Fig. 6, poly(DMAEMA-HA)

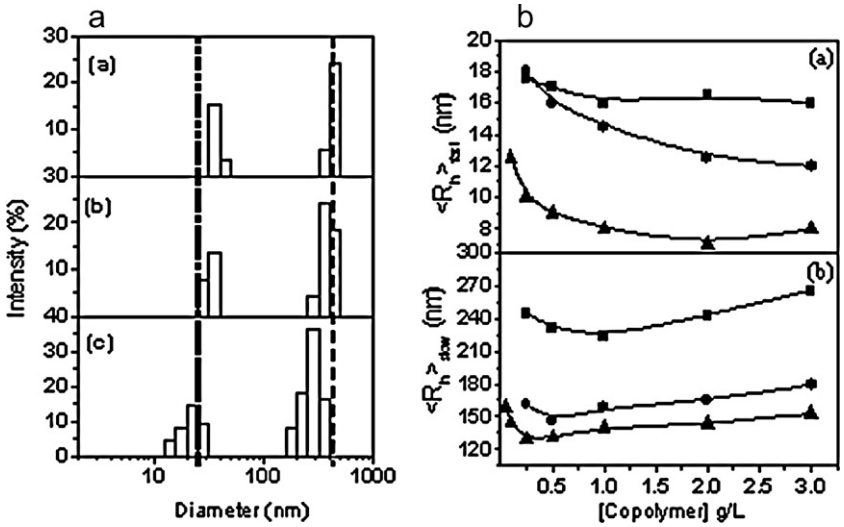

Fig. 6. (a) Intensity average distribution for 2 g/L copolymer in aqueous solution of pH 5 (with 100 mM NaCl) at 25 °C; (a) poly(DMAEMA-HA), (b) poly(DMAEMA-OA), (c) poly(DMAEMA-DA). Average hydrodynamic radius ($\langle R_h \rangle$) versus copolymer concentration (a) $\langle R_h \rangle_{fast,}$ (b) $\langle R_h \rangle_{slow}$; (■) poly(DMAEMA-HA), (●) poly(DMAEMA-OA), and (▲) poly(DMAEMA-DA).

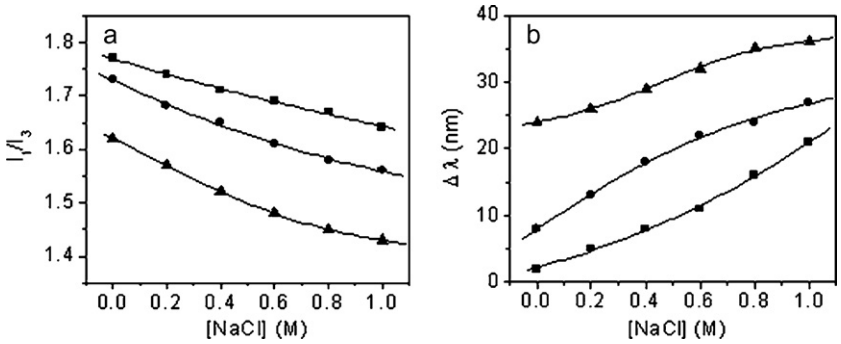

Fig. 7. (a) Plots of I_1/I_3 of pyrene and (b) emission maximum shift ($\Delta\lambda$) of NPN at different NaCl concentrations for 0.1 mg/mL copolymers; (■) poly(DMAEMA-HA), (●) poly(DMAEMA-OA), and (▲) poly(DMAEMA-DA).

has comparatively narrow and monodispersed size distribution with the population of a mean hydrodynamic diameter about 440 nm, which can be attributed to intermolecular association forming larger aggregates and the remaining population exhibited smaller size of about 34 nm, ascribed to an aggregate of small number of polymer chains. However, with the increase in chain length of the hydrophobe in the copolymer the mean diameter for both the population gradually decreases and the distribution becomes broad, indicating stronger hydrophobic association. Thus for poly(DMAEMA-DA), the average diameter reduces to ~300 and ~20 nm for the larger and smaller aggregates, respectively.

The relaxation rates (Γ) were also measured at various scattering angles in the range of 50–120° for the same concentration for all three HMPs. For both the fast and slow relaxation modes, Γ is plotted as a function of the scattering wave vector and are presented in Fig. S3 ("supplementary material"). The linear relationship of Γ with q^2 can be found for both modes. The straight lines pass through the origin, suggesting that the relaxation modes are virtually due to the translational diffusion of the scattering particles that are spherical in shape. Average hydrodynamic radius ($\langle R_h \rangle$) was calculated from the Stokes–Einstein relation using values of diffusion coefficient (D) estimated from the slope of the $\Gamma - q^2$ plots (for both the fast and slow modes). Values of $\langle R_h \rangle$ thus obtained for 1 g/L copolymer solution are listed in Table 2. The DLS measurements were also performed at different concentrations of the HMPs. The $\langle R_h \rangle$ determined at various concentrations are presented in Fig. 6(b). As seen, the radius corresponding to the fast decay mode ($\langle R_h \rangle_{fast}$) for poly(DMAEMA-HA) has a value of ~17 nm in dilute solution, which remained unaltered within the studied concentration range (Fig. 6(b)). However, with the increase in hydrophobe chain length, a decreasing trend of $\langle R_h \rangle_{fast}$ was observed at higher concentrations, showing a preference for effective interaction of hydrophobic groups. Thus, for poly(DMAEMA-DA) copolymer, the $\langle R_h \rangle_{fast}$ reduces to a value of ~8 nm from 13 nm. The hydrodynamic radius corresponding to the slow decay mode $\langle R_h \rangle_{slow}$, on the other hand, exhibits a different behavior. In dilute solution, a gradual decrease in $\langle R_h \rangle$ value followed by an increase at higher concentrations can be observed. Since in very dilute solution the HMPs are mostly hydrated, it is quite obvious to exhibit a much larger hydrodynamic radius. However, as soon as the polymer concentration increases, the inter-chain hydrophobic interaction favors micelle-like aggregate formation, which causes gradual decrease in hydrodynamic radius (Fig. 6(b)). Further, increase in hydrodynamic radius occurs probably due to the formation of multicore multipolymer aggregates.

3.7. Effect of salt concentration

Addition of salt causes changes in conformation of the polyelectrolyte. Usually, the electrolyte screens the ionic counterpart of the hydrophilic group and in turn facilitates the chain entanglement/packing. As a result, the aggregation through hydrophobic group becomes more favored. To investigate the effect of electrolyte for these copolymer conformations, we have performed the fluorometric titration using NPN and pyrene against sodium chloride concentration (a monovalent electrolyte) in 0.1 g/L copolymer. The plots of I_1/I_3 and $\Delta\lambda$ at different NaCl concentrations are shown in Fig. 7. Indeed, a gradual decrease of I_1/I_3 and increase of $\Delta\lambda$ value clearly demonstrate the profound association of the hydrophobic group caused by the shielding of the charges by the negatively charged Cl^- ions. The stronger association at high salt concentrations was further supported by the

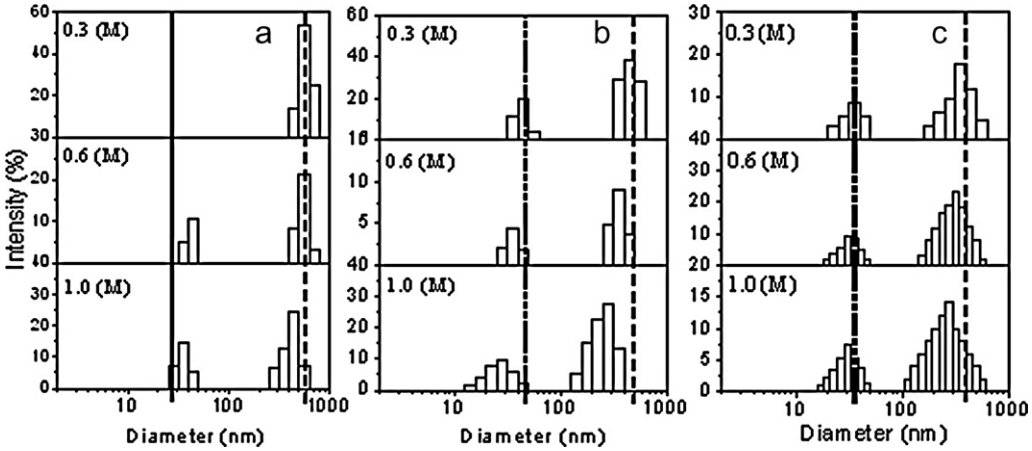

Fig. 8. Size distributions at different NaCl concentrations for 0.1 g/L (a) poly(DMAEMA-HA), (b) poly(DMAEMA-OA), and (c) poly(DMAEMA-DA) copolymer at 25 °C.

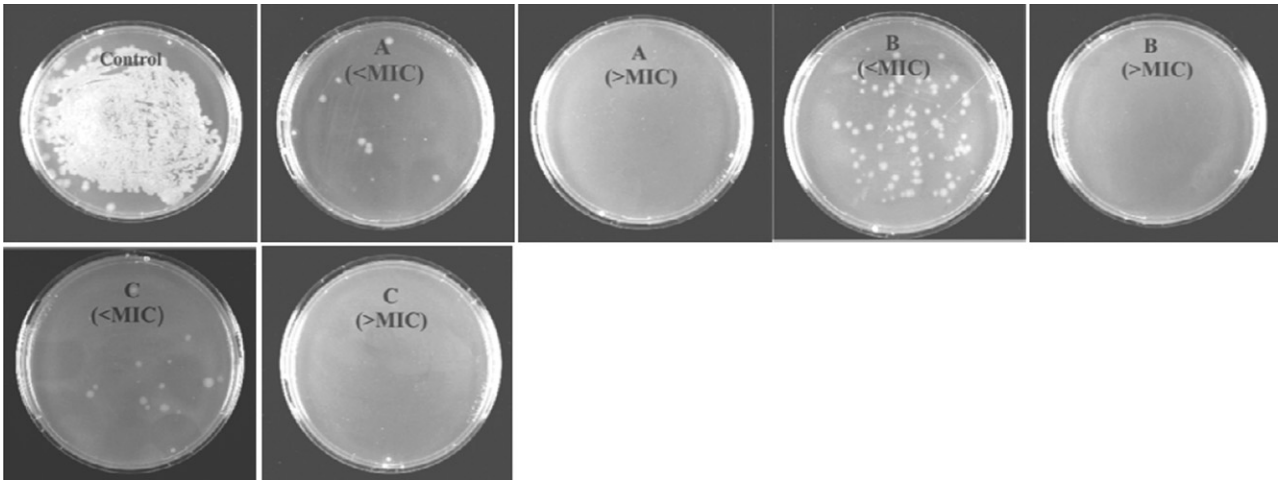

Fig. 9. Antibacterial assessment images of copolymers against *B. subtilis*; (A) poly(DMAEMA-HA), (B) poly(DMAEMA-OA), (C) poly(DMAEMA-DA).

measurement of DLS at the same copolymer concentration with three different NaCl concentrations. Intensity average size distributions of the aggregates in copolymer solutions at different NaCl (0.3, 0.6, 1.0 M) concentrations have been depicted in Fig. 8. It is observed that at low NaCl concentration (0.3 M), the copolymer poly(DMAEMA-HA) exhibits a monomodal distribution, whereas the HMPs poly(DMAEMA-OA) and poly(DMAEMA-DA) show a bimodal distribution with relatively larger diameters. However, with increasing NaCl concentration the distribution shifted to lower diameter range accompanied by a broadening the peak width, which confirms stronger hydrophobic association.

3.8. Effect of temperature

Thermal response of the copolymer micelles was investigated by fluorescence probe technique using DPH probe. Fluorescence anisotropy (r) of DPH was measured to investigate the effect of temperature on the micellar aggregates of the HMPs. Fig. S4 of "supplementary material" shows the variation of r as a function of temperature in 0.25 g/L copolymer solution. As observed, below 30 °C, the HMPs have high r-values, which suggest that the micelles are very rigid and stable at lower temperature. However, with increasing temperature they disintegrate into individual polymer chains, as reflected by the lower values of r at higher temperatures. The melting temperature is greater than 37 °C and increases in the order poly(DMAEMA-DA) > poly(DMAEMA-OA) > poly(DMAEMA-HA).

3.9. Antibacterial studies

The antibacterial activities of the copolymers poly(DMAEMA-HA), poly(DMAEMA-OA), and poly(DMAMEA-DA) were investigated against both the Gram-positive (*B. subtilis*) and Gram-negative bacteria (*E. coli*). The pictures of *B. subtilis* and *E. coli* before (control) and after treatment with the HMP (above and below MIC) are shown in Figs. 9 and 10. The minimum inhibitory concentrations (MIC) determined for each HMP against *B. subtilis* and *E coli* bacteria are summarized in Table 3. As seen, all the three HMPs under investigation have biocidal activity to Gram-positive bacteria *B. subtilis*, but in the case of Gram-negative bacteria *E. coli*, only poly(DMAEMA-HA), and poly(DMAEMA-OA) were active with MIC values 50 and 200 μg/mL, respectively. In contrast, poly(DMAEMA-DA) remained ineffective up to a concentration of 200 μg/mL. It has long been known that the chain length of hydrophobic unit

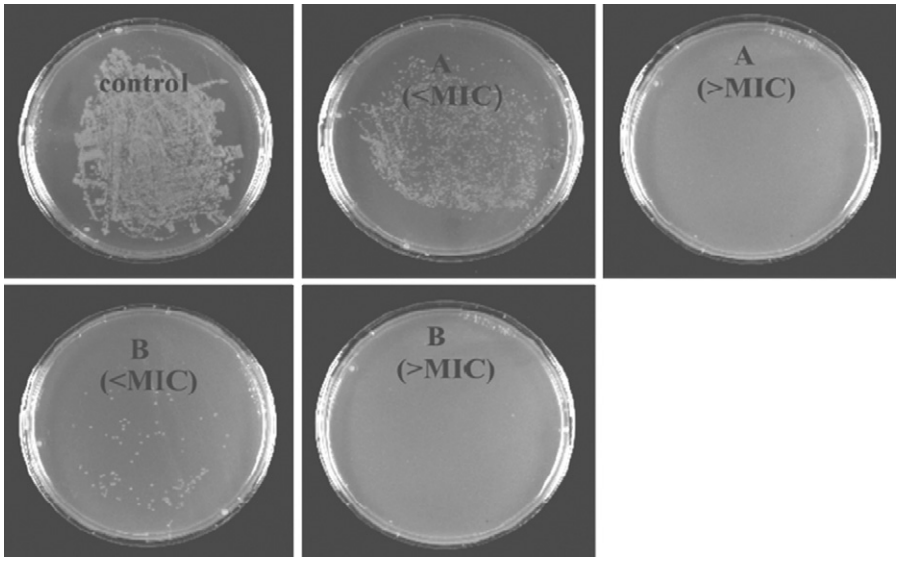

Fig. 10. Antibacterial assessment images of copolymers against *E.coli*; (A) poly(DMAEMA-HA), (B) poly(DMAEMA-OA).

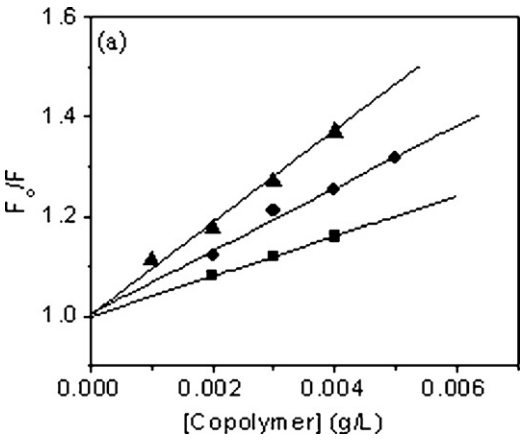

Fig. 11. Stern–Volmer plots for fluorescence quenching by copolymers. (■) poly(DMAEMA-HA), (●) poly(DMAEMA-OA), and (▲) poly(DMAEMA-DA).

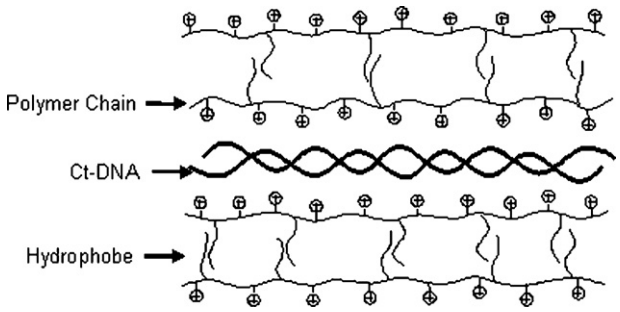

Chart 1. Structure of polymer-ct-DNA complex in solution.

in the cationic polymer plays a profound impact on the antibacterial activities (Ignatova et al., 2004; Kanazawa et al., 1993). To gain an effective antimicrobial action, an optimal range of alkyl chain is required (usually in the ranges of C_6 to C_{18}) as it can strongly bind to the cytoplasmic membrane of the bacteria which constitutes long-chain fatty acid with 12–20 carbon units through hydrophobic interaction (Domagk, 1935; Goodson et al., 1999; Franklin and Snow, 1981). Palermo and Kuroda reported recently the antibacterial activity of a library of amphiphilic random copolymers against *E. coli* containing DMAEMA monomers with various ratios of methylmethacrylate (C_1) (from 0 to 70 mol%) or butylmethacrylate (C_4) (from 0 to 40 mol%) (Palermo and Kuroda, 2009). They observed that the copolymers consisting of methyl (C_1) side chain as hydrophobic group with less than 20 mol% content failed to completely inhibit the growth of *E. coli* even up to 2000 μg/mL and reached a minimum of 242 μg/mL in the MIC value at 50% hydrophobe concentration and then increased as the hydrophobe concentration increased. In contrast, the copolymer with butyl (C_4) side chain as hydrophobic group were very effective in killing *E. coli* even at 12 mol% with MIC value 24 μg/mL. Similarly, in the case of polymethacrylamide random copolymer bearing protonated primary amine groups, the hexyl side chain containing copolymers impart more potent antimicrobial activity as compared to butyl side chain containing polymers at similar degree of polymerization and identical hydrophobe concentration (Palermo et al., 2009). To establish a relationship between the effect of hydrophobicity of the alkyl chain and their antimicrobial activities, Roy et al. (2008) further investigated a series of polymer on cellulosic filter using DMAEMA monomer which was subsequently quaternized with alkyl bromides of different chain lengths (C_8–C_{16}). They observed that cellulose graft copolymer that has been quaternized with a shorter alkyl chain (C_8) bromide is more effective against *E. coli* as compared to the cellulose graft copolymers quaternized with longer alkyl chain (C_{12} and C_{16}) bromides. Therefore, this may also be the case with poly(DMAEMA-DA) copolymer as it contains longer alkyl chain (C_{12}) compared to poly(DMAEMA-HA) (C_6) and poly(DMAEMA-OA) (C_8) copolymers. The excessive hydrophobicity resulted from poly(DMAEMA-DA) might possibly cause aggregation, reducing the number of cationic charges available to interact and thus making it difficult to kill the *E. coli*.

Further from the results of MIC values (Table 3), it can be concluded that these HMPs have a greater killing efficiency for Gram-positive bacteria than Gram-negative bacteria. This is in accordance with the result reported in the literature (Ignatova et al., 2004; Lenoir et al., 2006). Since, the Gram-positive bacteria have only peptidoglycan cell wall, the penetration for the cationic polyelectrolytes with hydrophobic group are easier. However, in the case of Gram-negative bacteria (*E. coli*), the cells are being surrounded by an additional outer membrane and hence, it is more difficult for macromolecules to diffuse through the cell wall. Furthermore, it is worth noting that among the three HMPs, poly(DMAEMA-OA) with octyl chain (C_8) as hydrophobic group has the strongest microbial efficiency with MIC value 20 μg/mL for Gram-positive *B. subtilis* which is just opposite to *E. coli.* Therefore, the poly(DMAEMA-OA) copolymer plausibly maintained the suitable balance of cationic charge with hydrophobicity for effective antimicrobial action against Gram-positive bacteria. In fact, like ours many other groups have also established that cationic polymers with octyl chain do possess optimal balance between the hydrophobicity and bacterial efficacy leading to highest activity (Ignatova et al., 2004; Lenoir et al., 2006; Roy et al., 2008).

Table 3
Minimum inhibition concentration of cationic polymers (μg/mL) and Stern–Volmer constant values for binding with ct-DNA of cationic polymers.

Copolymer	MIC (μg/mL)		K_{SV}[a] (L/g)	k_q[b] ($\times 10^{-9}$ L/g/s^1)
	B. subtilis	*E. coli*		
poly(DMAEMA-HA)	50	50	40	1.81
poly(DMAEMA-OA)	20	200	62.7	2.85
poly(DMAEMA-DA)	35	>200 μg/mL	88.7	4.02

[a] Stern–Volmer quenching constant.
[b] Bimolecular quenching constant.

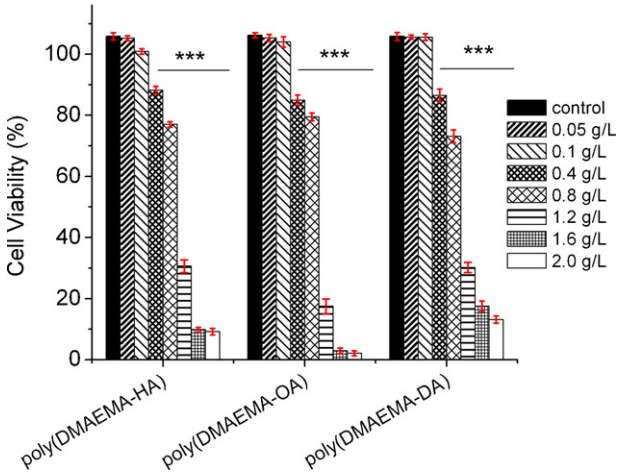

Fig. 12. MTT assay based fibroblast cell line 3T3 cell viability (in %) as a function of concentration for cationic copolymers at physiological pH (7.4). Significant difference is shown as $^{***}p < 0.001$ versus control. The bars indicate the means ± SD. ($n = 3$).

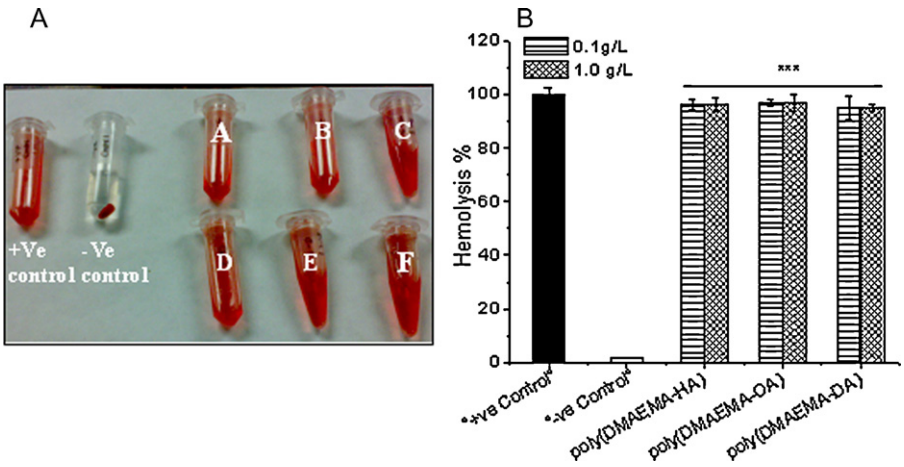

Fig. 13. (A) The picture of hemolytic assay for the copolymers, (B) % hemolysis of copolymers at 0.1 g/L and 1 g/L concentration at physiological pH (7.4). Significant difference is shown as $^{***}p < 0.001$ versus $^{-}$Ve control. The bars indicate the means ± SD. ($n = 3$).

3.10. Complexation with calf-thymus DNA

In an attempt to examine the complextation ability of the copolymers with DNA, fluorescence quenching studies were performed for the copolymers with calf-thymus DNA (ct-DNA) using EB as a fluorescent probe. The fluorescence spectra of EB (2 μM) and EB-ct-DNA ([ct-DNA] = 0.01 g/L) in absence and in the presence of different concentrations of poly(DMAEMA-DA) have been shown in Fig. S5 of "supplementary material". As observed, EB has a very weak emission band with an emission maximum of 590 nm in water, but in the presence of ct-DNA its emission intensity is greatly enhanced due to intercalation into the DNA strands. However, adding increasing concentration of copolymer poly(DMAEMA-DA) to EB-ct-DNA complex, the emission intensity of EB is significantly quenched, which suggests binding of poly(DMAEMA-DA) with ct-DNA.

The strength of binding of the HMP can be estimated by measuring the equilibrium constant of binding process:

$$\text{EB-ct-DNA} + \text{HMP} = \text{HMP-ct-DNA} + \text{EB} \quad (4)$$

The extent of fluorescence quenching at various polymer concentrations can be used to determine the Stern–Volmer (S–V) quenching constant (K), which is a measure of binding constant. To determine the K value, the fluorescence intensity of EB-ct-DNA was plotted against copolymer concentration (HMP) according to S–V equation (Lakowicz, 2006):

$$F_o/F = 1 + K\,[\text{HMP}] \quad (5)$$

where F_o and F stand for the fluorescence intensities in the absence and presence of polymer. The S–V plots for all the cationic HMPs employed in this study have been presented in Fig. 11. The binding constant K (Table 3) was obtained from the slope of the curve in the linear range. The data suggest that the binding of copolymers with longer hydrophobe chain is stronger than that with shorter hydrophobe chain. This means that the hydrophobes in the polymer backbone play a significant role in the binding process.

In order to understand the nature of binding of the cationic copolymers with ct-DNA, the circular dichroism (CD) spectra of DNA sample were measured in the presence of different concentrations of poly(DMAEMA-DA) as a representative HMP. The CD spectra have been shown in Fig. S6 of "supplementary material". The CD spectrum of DNA showed very little change upon binding of the copolymer, suggesting that the duplex structure of DNA remains almost unperturbed in the complexed state. This means that the ct-DNA-HMP binding is purely electrostatic in nature. In light of the above observations, the only way the increase of hydrophobe chain length can increase the binding ability of the HMP is through bilayer formation in solution. The ct-DNA becomes sandwiched (Chart 1) between two bilayers formed by the HMP. The appearance of turbidity in solution in the presence of larger amount of ct-DNA is an indication of bilayer formation. It is well known that the ability to form bilayer by amphiphilic molecules is increased with the increase of hydrophobic chain length. This means an increase of K value with the increase of the length of hydrophobe unit of the HMP. Such a complexation mode has been proposed by many authors for binding of phospholipids with DNA (Bhattacharya and Bajaj, 2009).

3.11. Cytotoxicity assay

The biocompatibility of the three amine-based HMPs was evaluated in terms of MTT assays. The cytotoxicity of the copolymers in the concentration range 0.05–2.0 g/L at physiological pH (7.4) was evaluated by measuring the viability of 3T3 cells using the MTT assay. As seen in Fig. 12, no significant toxicity was observed at low concentration for all three HMPs. However, with increase in concentration (>0.1 g/L) the cell viability significantly decreased and a much higher toxicity was observed at concentration above 1.2 g/L. Therefore, the HMPs at higher concentrations are toxic to this fibroblasts 3T3 cell line, while at lower concentration (i.e. the concentration well above MIC) they did not affect the cell growth and can be used for pharmaceutical applications. Unlike hemolytic activity, the cytotoxicity of cationic polymers depends differently. The greater number of cationic groups is considered to be more cytotoxic and the cytotoxicity can be reduced to some extent by increasing the hydrophobicity of cationic copolymer with either increasing the hydrophobic chain length or increasing the hydrophobe concentration. Palermo et al. recently investigated the cytotoxicity of methacrylamide based random copolymers bearing protonated primary amine and butyl or hexyl groups in the side chains of different substitution against human epithelial Hep-2 cells (Palermo et al., 2009). They observed that in contrast to unsubstituted polymer, the butyl or hexyl substituted polymer showed less cytoxicity up to 40 mol% hydrophobic substitutions which is quite consistent to our findings.

3.12. Hemocompatibility studies

Compatibility of the copolymers has also been tested with blood component red blood cells (RBCs). Hemolytic assays were

performed for all the three copolymers poly(DMAEMA-HA), poly(DMAEMA-OA), poly(DMAEMA-DA) in pH 7.4 (Hepes buffer, 20 mM). Freshly isolated BALB/c male mice RBC suspension (5%, v/v) was added to HEPES-buffered saline, 1% Triton X-100 and polymers with a final concentration of 0.1 and 1.0 mg/mL, and incubated for 60 min at 37 °C. The pictures associated to the hemolytic experiments are presented in Fig. 13(A). As seen although the HMPs are compatible to 3T3 fibroblast cell line, these are incompatible to RBC at both lower and higher concentration. This is also reflected by the % hemolysis presented in Fig. 13(B). Like antibacterial activity and cytotoxicity, the hemolytic activity is also strongly dependent on the chemical structures of polymers. Though the increase in hydrophobic side chain is believed to cause an increase in potency of antimicrobial effect of cationic polymers, it is found that increasing the hydrophobicity eventually lead to increased hemolysis. In this context, Palermo and Kuroda (2009) have recently investigated in more detail the hemolytic activity of amphiphilic random copolymers containing DMAEMA monomers with various ratios of methylmethacrylate (C_1) or butylmethacrylate (C_4). They observed that unlike poly(DMAEMA) homopolymer which is non-hemolytic even at high polymer concentration, a significant hemolysis was obtained for human red blood cells with HC_{50} value 2000 and 180 μg/mL for 19 mol% methyl and butyl hydrophobic content, respectively. Similar to their results, in the present investigation we also found that though all the three HMPs displayed a greater antibacterial activity, incorporation of longer alkyl chain results in a pronounced hydrophobic effect which caused a stronger hemolytic effect even at 100 μg/mL concentration.

4. Conclusions

In conclusion, we have synthesized three tertiary amine methacrylate based hydrophobically modified cationic copolymers of different alkyl chain lengths. In aqueous solution at pH 5.0, these polymers were found to form positively charged nanometer size aggregates above a critical concentration (CAC) through inter-polymer association as established by the fluorescence probe studies with NPN, pyrene, and DPH probes. The microenvironments of these aggregates are quite rigid and less polar and thus are capable of solubilizing hydrophobic drugs. Upon addition of salt the polarity of microenvironments decreases further and becomes more rigid. The polymeric nanoparticles were observed to be stable at physiological temperature (37 °C). Among the three HMPs, poly(DMAEMA-OA) was found to have the strongest microbial efficiency with MIC value 20 μg/mL for Gram-positive *B. subtilis*. However, no systematic order for the MIC value was observed for the HMPs with different chain lengths. All three HMPs were observed to strongly bind ct-DNA. The data suggest that the binding of HMPs with longer hydrophobe chain is stronger than that with shorter hydrophobe chain. It was observed that in the HMP-ct-DNA complex, the DNA duplex remains unchanged. Although the copolymers at higher concentrations (>1.2 g/L) are toxic to fibroblasts 3T3 cell line, at lower concentration (i.e. the concentration well above MIC), they did not affect the cell growth and can be used for pharmaceutical applications. However, the copolymers were found to be incompatible to red blood cells at both lower and higher concentrations, which restrict their use as i.v. injectible drug/gene carriers.

Acknowledgements

The authors gratefully acknowledge Basic Research in Nuclear Science (BRNS), Department of Atomic Energy (DAE) (grant no. 2006/37/17/BRNS/235), and Ministry of Human Resource Development (MHRD) of this work. PD thanks CSIR (09/081(0519)/2005-EMR-I) for a research fellowship. The authors are thankful to Dr. G. Ghosh, UGC-DAE Consortium for Scientific Research, BARC, Trombay, Mumbai 400 085, India for assistance with the DLS measurements.

Appendix A. Supplementary data

Supplementary data associated with this article can be found, in the online version, at doi:10.1016/j.ijpharm.2011.05.006.

References

Asokan, A., Cho, M.J., 2002. Exploitation of intracellular pH gradients in the cellular delivery of macromolecules. J. Pharm. Sci. 91, 903–913.
Bhattacharya, S., Bajaj, A., 2009. Advances in gene delivery through molecular design of cationic lipids. Chem. Commun., 4632–4656.
Domagk, G., 1935. A new class of disinfectants. Dtsch. Med. Wochenschr. 61, 829–832.
Dutta, P., Dey, J., Ghosh, G., Nayak, R.R., 2009. Self-association and microenvironment of random amphiphilic copolymers of sodium *N*-acryloyl-l-valinate and *N*-dodecylacrylamide in aqueous solution. Polymer 50, 1516–1525.
Franklin, T.J., Snow, G.A., 1981. Biochemistry of Antimicrobial Action. London, Chapman and Hall.
Georgiou, T.K., Vamvakaki, M., Phylactou, L.A., Patrickios, C.S., 2005. Synthesis, characterization, and evaluation as transfection reagents of double-hydrophilic star copolymers: effect of star architecture. Biomacromolecules 6, 2990–2997.
Goodson, B., Ehrhardt, A., Ng, S., Nuss, J., Johnson, K., Giedlin, M., Yamamoto, R., Moos, W.H., Krebber, A., Ladner, M., Giacona, M.B., Vitt, C., Winter, J., 1999. Characterization of novel antimicrobial peptoids. Antimicrob. Agents Chemother. 43, 1429–1434.
Gu, Z., Yuan, Y., He, J., Zhang, M., Ni, P., 2009. Facile approach for DNA encapsulation in functional polyion complex for triggered intracellular gene delivery: design, synthesis, and mechanism. Langmuir 25, 5199–5208.
Hoogeveen, N.G., Cohen Stuart, M.A., Fleer, G., 1996. Can charged (block co)polymers act as stabilisers and flocculants of oxides? Colloids Surf. A: Physicochem. Eng. Aspects 117, 77–88.
Huang, J., Koepsel, R.R., Murata, H., Wu, W., Lee, S.B., Kowalewski, T., Russell, A.J., Matyjaszewski, K., 2008. Nonleaching antibacterial glass surfaces via "Grafting Onto": the effect of the number of quaternary ammonium groups on biocidal activity. Langmuir 24, 6785–16785.
Huang, J., Murata, H., Koepsel, R.R., Russell, A.J., Matyjaszewski, K., 2007. Antibacterial polypropylene via surface-initiated atom transfer radical polymerization. Biomacromolecules 8, 1396–1399.
Ignatova, M., Voccia, S., Gilbert, B., Markova, N., Mercuri, P.S., Galleni, M., Sciannamea, V., Lenoir, S., Cossement, D., Gouttebaron, R., Jerome, R., Jerome, C., 2004. Synthesis of copolymer brushes endowed with adhesion to stainless steel surfaces and antibacterial properties by controlled nitroxide-mediated radical polymerization. Langmuir 20, 10718–10726.
Ikeda, T., Hirayama, H., Suzuki, K., Yamaguchi, H., Tazuke, S., 1986. Biologically active polycations, 6. Polymeric pyridinium salts with well-defined main chain structure. Die Makromolekulare Chemie 187, 333–340.
Ikeda, T., Yamaguchi, H., Tazuke, S., 1984. New polymeric biocides: synthesis and antibacterial activities of polycations with pendant biguanide groups. Antimicrob. Agents Chemother. 26, 139–144.
Kalyanasundaram, K., 1987. Photochemistry in Microheterogeneous Systems. Academic Press, New York, p. 40.
Kanazawa, A., Ikeda, T., Endo, T., 1993. Polymeric phosphonium salts as a novel class of cationic biocides. II. Effects of counter anion and molecular weight on antibacterial activity of polymeric phosphonium salts. J. Polym. Sci., Part A: Polym. Chem. 31, 1441–1447.
Katanasaka, Y., Ida, T., Asai, T., Shimizu, K., Koizumi, F., Maeda, N., Baba, K., Oku, N., 2008. Antiangiogenic cancer therapy using tumor vasculature-targeted liposomes encapsulating 3-(3,5-dimethyl-1H-pyrrol-2-ylmethylene)-1,3-dihydroindol-2-one, SU5416. Cancer Lett. 270, 260–268.
Kawabata, N., 1992. Capture of micro-organisms and viruses by pyridinium-type polymers and application to biotechnology and water purification. Prog. Polym. Sci. 17, 1–34.
Keely, S., Ryan, S.M., Haddleton, D.M., Limer, A., Mantovani, G., Murphy, E.P., Colgan, S.P., Brayden, D.J., 2009. Dexamethasone–pDMAEMA polymeric conjugates reduce inflammatory biomarkers in human intestinal epithelial monolayers. J. Controlled Release 135, 35–43.
Kenawy, E.R., Worley, S.D., Broughton, R., 2007. The chemistry and applications of antimicrobial polymers: a state-of-the-art review. Biomacromolecules 8, 1359–1384.
Kim, T.H., Jiang, H.L., Jere, D., Park, I.K., Cho, M.H., Nah, J.W., Choi, Y.J., Akaike, T., Cho, C.S., 2007. Chemical modification of chitosan as a gene carrier in vitro and in vivo. Prog. Polym. Sci. 32, 726–753.
Kurisawa, M., Yokoyama, M., Okano, T., 2000. Transfection efficiency increases by incorporating hydrophobic monomer units into polymeric gene carriers. J. Controlled Release 68, 1–8.

Lakowicz, J.R., 2006. Principles of Fluorescence Spectroscopy, 3rd ed. Plenum Press, New York.
Lakowicz, U., Breunig, M., Blunk, T., Göpferich, A., 2005. Polyethylenimine-based non-viral gene delivery systems. Eur. J. Pharm. Biopharm. 60, 247–266.
Lee, S.B., Koepsel, R.R., Morley, S.W., Matyjaszewski, K., Sun, Y., Russell, A.J., 2004. Permanent, nonleaching antibacterial surfaces. 1. Synthesis by atom transfer radical polymerization. Biomacromolecules 5, 877–882.
Lee, S.B., Russell, A.J., Matyjaszewski, K., 2003. ATRP synthesis of amphiphilic random, gradient, and block copolymers of 2-(dimethylamino)ethyl methacrylate and *n*-butyl methacrylate in aqueous media. Biomacromolecules 4, 1386–1393.
Lenoir, S., Pagnoulle, C., Detrembleur, C., Galleni, M., Jerome, R., 2005. Antimicrobial activity of polystyrene particles coated by photo-crosslinked block copolymers containing a biocidal polymethacrylate. e-Polymers 074, 1–11.
Lenoir, S, Pagnoulle, C., Detrembleur, C., Galleni, M., Jerome, R., 2006. New antibacterial cationic surfactants prepared by atom transfer radical polymerization. J. Polym. Sci., Part A: Polym. Chem. 44, 1214–1224.
Lv, H., Zhang, S., Wang, B., Cui, S., Yan, J., 2006. Toxicity of cationic lipids and cationic polymers in gene delivery. J. Controlled Release 114, 100–109.
Malafaya, P.B., Silva, G.A., Reis, R.L., 2007. Natural-origin polymers as carriers and scaffolds for biomolecules and cell delivery in tissue engineering applications. Adv. Drug. Deliv. Rev. 59, 207–233.
Merle, Y., 1987. Synthetic polyampholytes. 5. Influence of nearest-neighbor interactions on potentiometric curves. J. Phys. Chem. 91, 3092–3098.
Morishima, Y., Kobayashi, T., Nozakura, S., 1989. Amphiphilic polyelectrolytes with various hydrophobic groups: intramolecular hydrophobic aggregation in aqueous solution. Polym. J. (Tokyo) 21, 267–274.
Mitra, R.N., Shome, A., Paul, P., Das, P.K., 2009. Antimicrobial activity, biocompatibility and hydrogelation ability of dipeptide-based amphiphiles. Org. Biomol. Chem. 7, 94–102.
Mohanty, A., Dey, J., 2007. Effect of the headgroup structure on the aggregation behavior and stability of self-assemblies of sodium *N*-[4-(*n*-dodecyloxy)benzoyl]-l-aminoacidates in water. Langmuir 23, 1033–1040.
Niwa, M., Morikawa, M., Yagi, K., Higashi, N., 2002. Interaction between polylysine monolayer and DNA at the air–water interface. Int. J. Biol. Macromol. 30, 47–54.
Nonaka, T., Hua, L., Ogata, T., Kurihara, S., 2003. Synthesis of water-soluble thermosensitive polymers having phosphonium groups from methacryloyloxyethyl trialkyl phosphonium chlorides–*N*-isopropylacrylamide copolymers and their functions. J. Appl. Polym. Sci. 87, 386–393.
Palermo, E.F., Kuroda, K., 2009. Chemical structure of cationic groups in amphiphilic polymethacrylates modulates the antimicrobial and hemolytic activities. Biomacromolecules 10, 1416–1428.
Palermo, E.F., Sovadinova, I., Kuroda, K., 2009. Structural determinants of antimicrobial activity and biocompatibility in membrane-disrupting methacrylamide random copolymers. Biomacromolecules 10, 3098–3107.
Park, T.G., Jeong, J.H., Kim, S.H., 2006. Current status of polymeric gene delivery systems. Adv. Drug. Deliv. Rev. 58, 467–486.
Pitt, W.G., Mcbride, M.O., Lunceford, J.K., Roper, R.J., Sagers, R.D., 1994. Ultrasonic enhancement of antibiotic action on gram-negative bacteria. Antimicrob. Agents Chemother. 38, 2577–2582.
Pradny, M., Sevcik, S., 1985. Precursors of hydrophilic polymers, 3. The potentiometric behaviour of isotactic and atactic poly(2-dimethylaminoethyl methacrylate) in water/ethanol solutions. Makromol. Chem. 186, 111–121.
Rawlinson, L.B., Ryan, S.M., Mantovani, G., Syrett, J.A., Haddleton, D.M., Brayden, D.J., 2010. Antibacterial effects of poly(2-(dimethylamino ethyl)methacrylate) against selected gram-positive and gram-negative bacteria. Biomacromolecules 11, 443–453.
Roy, D., Knapp, J.S., Guthrie, J.T., Perrier, S., 2008. Antibacterial cellulose fiber via RAFT surface graft polymerization. Biomacromolecules 9, 91–99.
Roy, S., Mohanty, A., Dey, J., 2005. Microviscosity of bilayer membranes of some *N*-acylamino acid surfactants determined by fluorescence probe method. Chem. Phys. Lett. 414, 23–27.
Roy, S., Das, P.K., 2008. Antibacterial hydrogels of amino acid-based cationic amphiphiles. Biotechnol. Bioeng. 100, 756–764.
Rungsardthong, U., Deshpande, M., Bailey, L., Vamvakaki, M., Armes, S.P., Garnett, M.C., Stolnik, S., 2001. Copolymers of amine methacrylate with poly(ethylene glycol) as vectors for gene therapy. J. Controlled Release 73, 359–380.
Tan, J.F., Too, H.P., Hatton, T.A., Tam, K.C., 2006. Aggregation behavior and thermodynamics of binding between poly(ethylene oxide)-block-poly(2-(diethylamino)ethyl methacrylate) and plasmid DNA. Langmuir 22, 3744–3750.
Tashiro, T., 2001. Antibacterial and bacterium adsorbing macromolecules. Macromol. Mater. Eng. 286, 63–87.
Van de Wetering, P., Cherng, J.Y., Talsma, H., Hennink, W.E., 1997. Relation between transfection efficiency and cytotoxicity of poly(2-(dimethylamino)ethyl methacrylate)/plasmid complexes. J. Controlled Release 49, 59–69.
Wetering, P.V.D., Cherng, J.Y., Talsma, H., Crommelin, D.J.A., Hennink, W.E., 1998. 2-(dimethylamino)ethyl methacrylate based (co)polymers as gene transfer agents. J. Controlled Release 53, 145–153.
Wetering, P.V.D., Moret, E.E., Nieuwenbroek, N.M.E., Steenbergen, M.J.V., Hennink, W.E., 1999. Structure-activity relationships of water-soluble cationic methacrylate/methacrylamide polymers for nonviral gene delivery. Bioconjug. Chem. 10, 589–597.
Zhang, F., Wu, Q., Chen, Z., Zhang, M., Lin, X., 2008. Hepatic-targeting microcapsules construction by self-assembly of bioactive galactose-branched polyelectrolyte for controlled drug release system. J. Colloid Interface Sci. 317, 477–484.
Zhu, S., Yang, N., Zhang, D., 2009. Poly(*N*,*N*-dimethylaminoethyl methacrylate) modification of activated carbon for copper ions removal. Mater. Chem. Phys. 113, 784–789.